

## Facile Synthesis of Cobalt Vanadium Oxides and Their Applications in Lithium Batteries

Yan Tang, Jiang Zhou, Jing Liu, Lingxin Liu, Shuquan Liang\*

School of Material Science and Engineering, Central South University, Changsha 410083, China

\*E-mail: [sqliang\\_csu@126.com](mailto:sqliang_csu@126.com)

Received: 26 November 2012 / Accepted: 18 December 2012 / Published: 1 January 2013

---

Cobalt vanadium oxides ( $\text{CoV}_2\text{O}_6$  and  $\text{Co}_2\text{V}_2\text{O}_7$ ) have been one-step synthesized by a soft chemistry route without any templates. The as-prepared materials were characterized by a variety of analytical techniques, including X-ray diffraction (XRD), Scanning electron microscopy (SEM), Energy dispersive X-ray spectroscopy (EDS), Fourier-transform infrared spectroscopy (FT-IR). The XRD patterns showed that the as-prepared materials are of high crystallinity and high purity. The SEM images showed that the  $\text{Co}_2\text{V}_2\text{O}_7$  material is very uniform and well-separated, with diameters around 1  $\mu\text{m}$ . The electrochemical performances were also investigated and the results show that the  $\text{CoV}_2\text{O}_6$  material can deliver a high initial discharge capacity of 1243  $\text{mAh g}^{-1}$  at the current density of 20  $\text{mA g}^{-1}$  and the  $\text{Co}_2\text{V}_2\text{O}_7$  material exhibits a high initial discharge capacity of 949  $\text{mAh g}^{-1}$  even at a large current density as high as 500  $\text{mA g}^{-1}$ .

---

**Keywords:**  $\text{CoV}_2\text{O}_6$ ;  $\text{Co}_2\text{V}_2\text{O}_7$ ; soft chemistry, anode material; lithium battery

### 1. INTRODUCTION

Owing to the superior performances including high power and energy density, long cycle life, safety and no memory effect, rechargeable lithium-ion batteries (LIBs) have their wide applications in portable electronics such as cell phones, laptop computers, digital cameras and electric vehicles, power tools[1-5]. A rechargeable LIB is typically composed of a cathode and an anode. Generally, the graphite, with the favorable low voltage for the lithium-ion intercalation/de-intercalation and a long cycle life, were used as the anode of the commercial LIBs [6,7]. However, the graphite anode materials used in rechargeable LIBs cannot meet the need of large-scale batteries in the future because their low capacity (about 372  $\text{mAh g}^{-1}$ ) and poor cyclability [8]. To alleviate the problem, considerable efforts should be devoted to find out alternative anode materials to replace graphite anode.

In recent years, transition-metal vanadium-based oxides have attracted extensive attentions and they have wide applications in the fields such as catalysts, chemistry sensors, optical devices, lithium battery electrode materials for their special physical, chemical properties [9-13]. Cobalt-based vanadates are such typical of vanadium oxides. Owing to their novel electrochemical, catalytic, and magnetic properties, various efforts have been devoted to develop new approaches for the synthesis of  $\text{CoV}_2\text{O}_6$  nano/microstructures, such as solid-state reaction method [14, 15], coprecipitation method [16], 'chimie douce' method [17] and hydrothermal method [18, 19]. According to previous reports, the anode made of  $\text{CoV}_2\text{O}_6$  exhibits a much higher initial discharge capacity than graphite anode material, indicating to be potential anode material for lithium ion batteries. Tarascon and his co-workers [16, 17] have synthesized the  $\text{CoV}_2\text{O}_6$  material and the Li uptake/removal mechanism was discussed. Zhou et al. [18] have synthesized the single-crystalline  $\text{CoV}_2\text{O}_6 \cdot 2\text{H}_2\text{O}$  nanobelts and its dehydrated salt  $\text{CoV}_2\text{O}_6$  exhibit the initial discharge capacity of  $980 \text{ mAh} \cdot \text{g}^{-1}$  and  $675 \text{ mAh} \cdot \text{g}^{-1}$ , respectively. Ma et al. [19] report a facile hydrothermal route for the synthesis of  $\text{CoV}_2\text{O}_6$  nanowires and microrods and their growth mechanism was investigated.

Due to their interesting structural features, with the crystallize in a monoclinic system of space group  $\text{P2}_1/\text{c}$ , the  $\text{Co}_2\text{V}_2\text{O}_7$  material showing interesting magnetic and electrochemical behaviors have attracted more and more concerns and they have an active field in solid-state chemistry and physics [13,16,20,21]. He et al. [20] have synthesized the single crystals of  $\text{Co}_2\text{V}_2\text{O}_7$  using the flux method in a closed crucible and investigated the magnetic properties. Sánchez-Andújar et al. [21] have synthesized  $\text{Co}_2\text{V}_2\text{O}_7$  by the ceramic method and their dielectric behaviors are reported. Baudrin et al. [16] have synthesized  $\text{Co}_2\text{V}_2\text{O}_7$  by a coprecipitation process and their electrochemical properties are measured. To the best of our knowledge, the electrochemical properties of  $\text{Co}_2\text{V}_2\text{O}_7$  are rarely reported.

In this paper, we have described a facile one-step soft chemistry method for the preparation of  $\text{CoV}_2\text{O}_6$  and  $\text{Co}_2\text{V}_2\text{O}_7$  materials without any templates or catalyts. The crystal structure and morphologies of  $\text{CoV}_2\text{O}_6$  and  $\text{Co}_2\text{V}_2\text{O}_7$  microstructures are evaluated and their electrochemical performances were tested as anode materials for lithium batteries.

## 2. EXPERIMENTAL SECTIONS

All chemicals used in our experiments are of analytical purity and used as received without further purification. Cobalt vanadium oxides ( $\text{CoV}_2\text{O}_6$ ,  $\text{Co}_2\text{V}_2\text{O}_7$ ) were prepared using  $\text{V}_2\text{O}_5$  (99.0%),  $\text{C}_2\text{H}_2\text{O}_4 \cdot 2\text{H}_2\text{O}$  (99.5%) and  $\text{Co}(\text{NO}_3)_2 \cdot 6\text{H}_2\text{O}$  (99.0%) as starting materials. Vanadyl oxalic ( $\text{VOC}_2\text{O}_4$ ) as vanadium source was prepared using a soft chemistry method, which was similar to our previous reports [22-25].

$\text{CoV}_2\text{O}_6$ . In a typical procedure,  $\text{V}_2\text{O}_5$  and  $\text{C}_2\text{H}_2\text{O}_4 \cdot 2\text{H}_2\text{O}$  in a molar ration of 1:3 were added into actively stirred de-ionized water at room temperature until the color of the solution changed from yellow to blue, indicating that the  $\text{VOC}_2\text{O}_4$  was formed. A stoichiometric amount of  $\text{Co}(\text{NO}_3)_2 \cdot 6\text{H}_2\text{O}$  was put into a beaker with 20mL of de-ionized water and magnetically stirred at room temperature until the solution clarified. Then the  $\text{Co}(\text{NO}_3)_2 \cdot 6\text{H}_2\text{O}$  solution was slowly added into the above synthesized  $\text{VOC}_2\text{O}_4$  solution and vigorously stirred for 2h at  $60^\circ\text{C}$ . Then the solution was dried at

60°C for 18h. After that, the as-obtained solid mixture was calcined at 700°C in air for 5h and the final product obtained.

$\text{Co}_2\text{V}_2\text{O}_7$ . The  $\text{Co}_2\text{V}_2\text{O}_7$  material was prepared by a similar process for the synthesis of  $\text{CoV}_2\text{O}_6$ , except the temperature of calcination was extended to 750°C.

The crystal structures of the as-prepared materials were studied by X-ray diffraction (XRD, Rigaku D/max2500 XRD with Cu K $\alpha$  radiation,  $\lambda=1.54178$  Å). The morphologies and sizes of the prepared products were characterized by Scanning electron microscopy (SEM, FEI Sirion200) equipped with an Energy dispersive X-ray spectroscopy (EDS) detector. The Fourier-transform infrared spectroscopy (FT-IR) spectrums were obtained within the 400-4000  $\text{cm}^{-1}$  region on a Nicolet 6700 FTIR spectrometer using KBr pellets.

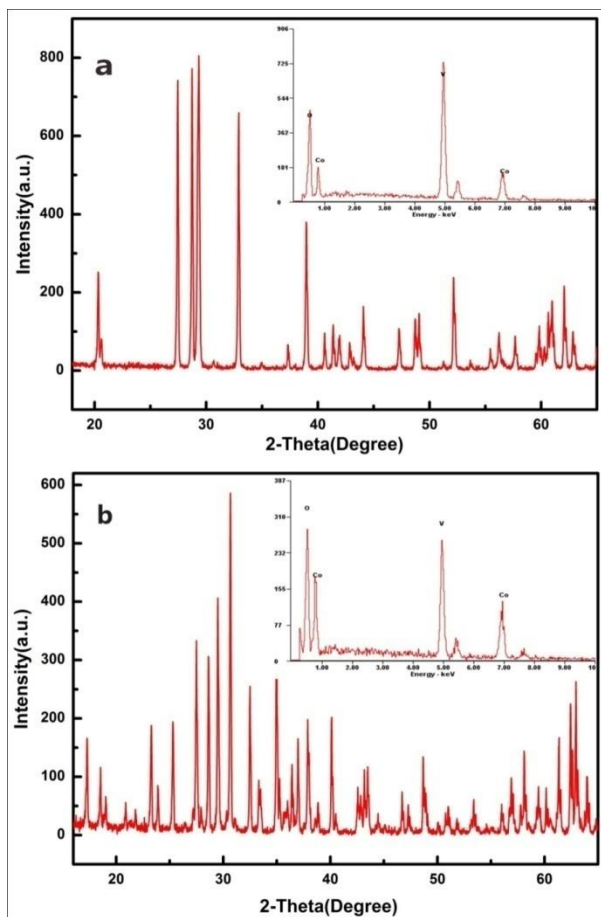
Electrochemical experiments were carried out via a coin battery cell (2025 type coin cell). To prepare the cathode, a mixture of the as-prepared materials ( $\text{CoV}_2\text{O}_6$  or  $\text{Co}_2\text{V}_2\text{O}_7$ ), acetylene black, and polyvinylidene fluoride (PVDF) binder in a weight ratio of 80 : 10 : 10 was dispersed in a N-methyl-2-pyrrolidone (NMP) solution to make a slurry. The slurry was coated on a copper foil and dried in a vacuum oven at 90°C overnight prior to coin-cell assembly. The cells were assembled in a glove box (Mbraun, Germany) filled with ultrahigh purity argon using polypropylene membrane as the separator, Li metal as the anode, and 1-M  $\text{LiPF}_6$  in ethylene carbonate/dimethyl carbonate (EC/DMC) (1 : 1 EC:DMC v/v) as the electrolyte. The galvanostatic charge/discharge performances of the electrodes were evaluated at room temperature using an Land Battery Tester (Land CT 2001A, Wuhan, China) within the voltage range of 0.01V-3 V (vs.  $\text{Li/Li}^+$ ).

### 3. RESULTS AND DISCUSSION

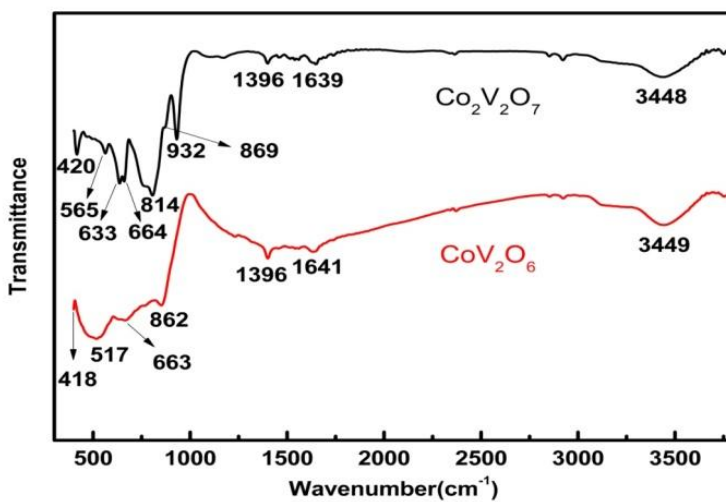
The purities of the as-prepared  $\text{CoV}_2\text{O}_6$  and  $\text{Co}_2\text{V}_2\text{O}_7$  materials were confirmed by X-ray diffraction (XRD) spectrometry. As shown in Fig. 1a, all the diffraction peaks can be readily assigned to the pure  $\text{CoV}_2\text{O}_6$  phase [space group: C, JCPDS Card No.38-0090]. No peaks of any other phases have been detected, indicating high purity of the material. Moreover, the Energy dispersive X-ray spectroscopy (EDS) analysis (inset Fig. 1a) of the product shows a typical spectrum of  $\text{CoV}_2\text{O}_6$ , showing the elemental ratio of Co and V with the molar ratio of 1:2 approximately and no other metal elements except for Co and V were confirmed, which agrees well with the result of XRD analysis. As shown in Fig. 1b, we can see that most of the peaks in the XRD pattern can be indexed to the pure  $\text{Co}_2\text{V}_2\text{O}_7$  phase [space group:  $\text{P}2_1/\text{c}$  (14), JCPDS Card No.29-0519]. The EDS investigation taken from the material indicates the presence of Co, V, and O elements are close to the ratio of 2:2:7, which is confirmed well with the theoretical value, indicating that the material is of high purity. Furthermore, we can see that both the peaks are strong and narrow in Fig. 1a and 1b, which demonstrates the high crystallinity of the as-prepared materials.

Fig.2 shows the Fourier-transform infrared spectroscopy (FT-IR) spectrums of the as-prepared  $\text{CoV}_2\text{O}_6$  and  $\text{Co}_2\text{V}_2\text{O}_7$  materials. In the FTIR spectrum of  $\text{Co}_2\text{V}_2\text{O}_7$ , the bands at 932 and 814  $\text{cm}^{-1}$  can be attributed to the symmetric and asymmetric stretching of  $\text{VO}_4$  units, respectively [26]. The

absorption bands at  $862\text{ cm}^{-1}$  of  $\text{CoV}_2\text{O}_6$  may be assigned to  $\text{V}=\text{O}$  stretching mode while the  $\text{Co}_2\text{V}_2\text{O}_7$  locates at  $869\text{ cm}^{-1}$ [27].



**Figure 1.** XRD patterns of the as-prepared materials (a)  $\text{CoV}_2\text{O}_6$  and (b)  $\text{Co}_2\text{V}_2\text{O}_7$ ; the inset shows the typical EDS spectrums of the materials, respectively.



**Figure 2.** FT-IR spectrums of the as-prepared  $\text{CoV}_2\text{O}_6$  and  $\text{Co}_2\text{V}_2\text{O}_7$  materials.

Both the bands of  $\text{CoV}_2\text{O}_6$  and  $\text{Co}_2\text{V}_2\text{O}_7$  in the region of  $500\text{-}700\text{ cm}^{-1}$  are due to the V-O-V bonds corresponding to the asymmetric or symmetric stretches [26]. And the bands at around  $420\text{ cm}^{-1}$  can be assigned to the stretching of Co-O modes. The bands at  $1396\text{ cm}^{-1}$  can be ascribed to the residue of nitrate from the reactant and the bands around  $3448$  and  $1639\text{ cm}^{-1}$  show the presence of the free water with the stretching of O-H and flexural vibrations of the O-H, respectively [27].

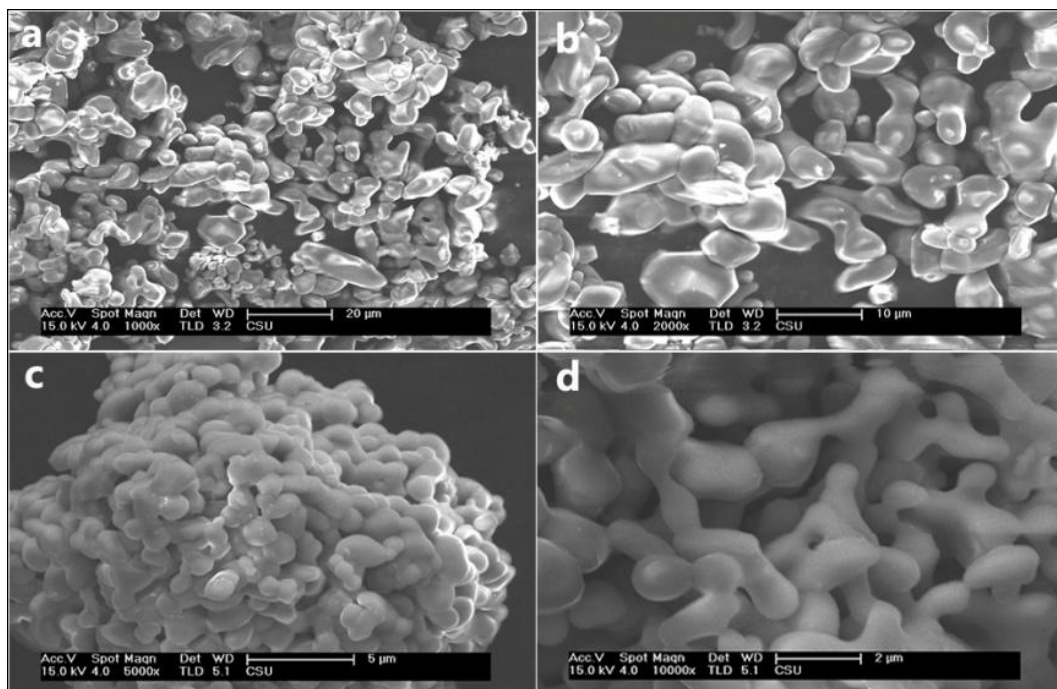


**Figure 3.** SEM images of different magnifications for the as-prepared materials (a,b)  $\text{CoV}_2\text{O}_6$  and (c,d)  $\text{Co}_2\text{V}_2\text{O}_7$ .

The morphologies of the as-prepared  $\text{CoV}_2\text{O}_6$  and  $\text{Co}_2\text{V}_2\text{O}_7$  materials were examined by scanning electron micrographs (SEM). Fig. 3a and 3b show the typical SEM images of the  $\text{CoV}_2\text{O}_6$  materials. The SEM images reveals that the  $\text{CoV}_2\text{O}_6$  materials consists of a large particle size of about 3 to 8  $\mu\text{m}$ , mixed with some small particles with the sizes about 500 nm. Moreover, the particles seem to be some agglomerated oddment. Fig. 3c and 3d show the typical SEM images of the  $\text{Co}_2\text{V}_2\text{O}_7$  powders of different magnifications. As we can see from Fig. 3c and 3d, with the sizes around 1  $\mu\text{m}$ , the particles are very uniform and their surfaces are smooth. Furthermore, ample space between the particles can be clearly observed. Compared to the  $\text{CoV}_2\text{O}_6$  material, the  $\text{Co}_2\text{V}_2\text{O}_7$  material with much smaller particles separated well with each other, was expected to have better electrochemical performances.

Fig. 4 shows the first discharge curve of the electrodes made of the as-prepared  $\text{CoV}_2\text{O}_6$  material at different current densities. As we can see from Fig. 4, the  $\text{CoV}_2\text{O}_6$  material exhibits a high initial discharge capacity of  $1243\text{ mAh g}^{-1}$ , which is much higher than that of the  $\text{CoV}_2\text{O}_6$  nanorods ( $675\text{ mAh g}^{-1}$ ) [18]. And we can see a sharply drop to around 0.7 V (vs.  $\text{Li/Li}^+$ ) from the beginning of the discharge curve, indicating that there is no reaction with lithium at these voltages, which may be

ascribed to the decomposition of electrolyte and formation of solid electrolyte interface (SEI) [28]. A distinct plateau, corresponding to the capacity of  $300 \text{ mA g}^{-1}$ , is observed at  $0.4 \text{ V}$  (vs.  $\text{Li/Li}^+$ ), then a gradual voltage decrease down to  $0.01 \text{ V}$  (vs.  $\text{Li/Li}^+$ ) with the capacity of  $900 \text{ mA g}^{-1}$ .

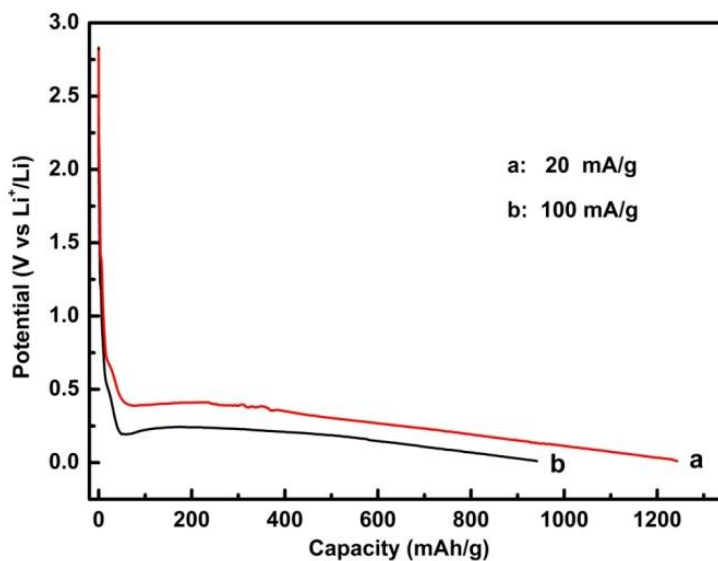


**Figure 4.** First discharge curves of the electrodes made from the as-prepared  $\text{CoV}_2\text{O}_6$  material at different current densities.

The rate performance test shows that it can deliver an initial specific discharge capacity of  $941 \text{ mAh g}^{-1}$  at the current density of  $100 \text{ mA g}^{-1}$ , with the discharge voltage being a little slower than that of the current density of  $20 \text{ mA g}^{-1}$ .

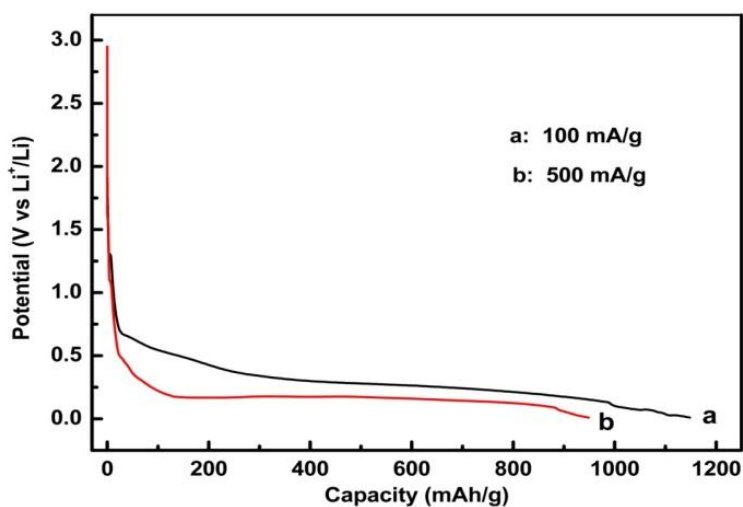


**Figure 5.** First discharge curves of the electrodes made from the as-prepared  $\text{Co}_2\text{V}_2\text{O}_7$  material at different current densities.

The first discharge curve of the as-prepared  $\text{Co}_2\text{V}_2\text{O}_7$  material was also measured and the results are shown in Fig.5. The electrochemical behavior is similar to the as-prepared  $\text{CoV}_2\text{O}_6$  material with a rapid drop of potential at the beginning of the discharge curves. A distinct plateau at around 0.3V (vs.  $\text{Li}/\text{Li}^+$ ) is clearly observed and a high initial specific discharge capacity of  $1148 \text{ mAh g}^{-1}$  is obtained at the current density of  $100 \text{ mA g}^{-1}$ , which is much higher than that of the as-prepared  $\text{CoV}_2\text{O}_6$  material. It is amazing that it can demonstrate the first discharge of  $949 \text{ mAh g}^{-1}$  with a low plateau at around 0.15V (vs.  $\text{Li}/\text{Li}^+$ ) at the current density of  $500 \text{ mA g}^{-1}$ . The high initial discharge capacity in compared to the  $\text{CoV}_2\text{O}_6$  material is mainly ascribed to its interesting structural features and the samples' morphology, and the results are similarly to the previous report [16]. The well-separated smaller particles in size of the  $\text{Co}_2\text{V}_2\text{O}_7$  material make it achieve high initial capacity and high rate capability. The particles with ample space between each other are beneficial to the easier penetration of the electrolyte leading to more reaction sites on the surface, and more flexible for lithium intercalation/de-intercalation, such the better electrochemical performance can be achieved [29, 30].

The Li uptake/removal mechanism of the as-prepared  $\text{CoV}_2\text{O}_6$  and  $\text{Co}_2\text{V}_2\text{O}_7$  materials are different from a classical intercalation process [16, 17]. Their abilities to take up large amounts of lithium ions, based on strong oxygen Li interactions ('Li-O' bonds) [16, 31], are associated with the high initial lithium storage capacity, which are about three times higher than the classical graphite. An interesting discovery is that both the materials can achieve high capacity under the potential of 0.5V (vs.  $\text{Li}/\text{Li}^+$ ), when they use as the anode materials in lithium-ion battery, a high open circuit voltage can be achieved. Moreover, no special equipments are required for the preparation of the materials and the method can be easily scale-up for large quantity production, and this method can be used to the synthesis of the other materials. What's more, the materials obtained in our new method can be used in the other fields such as catalysts, chemistry sensors, optical devices, et al.

#### 4. CONCLUSION

In summary, the  $\text{CoV}_2\text{O}_6$  and  $\text{Co}_2\text{V}_2\text{O}_7$  materials of high crystallinity and high purity have been large scale synthesized and characterized. The results of electrochemical measurement indicate that both the as-prepared  $\text{CoV}_2\text{O}_6$  and  $\text{Co}_2\text{V}_2\text{O}_7$  materials can deliver a high initial discharge capacity and better rate capacity. Further work should be done to improve the reversible capacity such as reducing the particle size [32], carbon coated [33] and so on.

#### ACKNOWLEDGMENT

This work was supported by Creative research group of National Natural Science Foundation of China (No. 50721003) and Mittal Student Innovation Program of Central South University (No. 11MX23).

#### References

1. J.M. Tarascon, M. Armand, *Nature* 414 (2001) 359.

2. A. Yoshino, *Angew. Chem. Int. Ed.* 51 (2012) 2.
3. J.B. Goodenough, Y. Kim, *Chem. Mater.* 22 (2010) 587.
4. H.K. Song, K.T. Lee, M.G. Kim, L.F. Nazar, J. Cho, *Adv. Funct. Mater.* 20 (2010) 3818.
5. S.T. Myung, K. Amine, Y.K. Sun, *J. Mater. Chem.* 20 (2010) 7074.
6. H. Li, Z.X. Wang, L.Q. Chen, X.J. Huang, *Adv. Mater.* 21 (2009) 4593.
7. C.L. Fan, H. Chen, *J. Mater. Sci.* 46 (2011) 2140.
8. J. Jiang, Y.Y. Li, J.P. Liu, X.T. Huang, *Nanoscale* 3 (2011) 45.
9. H.F. Shi, Z.S. Li, J.H. Kou, J.H. Ye, Z.G. Zou, *J. Phys. Chem. C* 115 (2011) 145.
10. L.Q. Mai, L. Xu, Q. Gao, C.H. Han, B. Hu, Y.Q. Pi, *Nano. Lett.* 10 (2010) 2604.
11. H. Ma, S.Y. Zhang, W.Q. Ji, Z.L. Tao, J. Chen, *J. Am. Chem. Soc.* 130 (2008) 5361.
12. A.J. Xu, Q. Lin, M.L. Jia, B. Zhaorigetu, *React. Kinet. Catal. Lett.* 93 (2008) 273.
13. S.J. Lei, K.B. Tang, Y. Jin, C.H. Chen, *Nanotechnology* 18 (2007) 175605.
14. Z.Z. He, J.I. Yamaura, Y. Ueda, W.D. Cheng, *J. Am. Chem. Soc.* 131 (2009) 7554.
15. M. Lenertz, J. Alaria, D. Stoeffler, S. Colis, A. Dinia, *J. Phys. Chem. C* 115 (2011) 17190.
16. E. Baudrin, S. Laruelle, S. Denis, M. Touboul, J.M. Tarascon, *Solid State Ionics* 123 (1999) 139.
17. S. Denis, E. Baudrin, F. Orsini, G. Ouyard, M. Touboul, J.M. Tarascon, *J. Power Sources* 81 (1999) 79.
18. H.Y. Zhou, Y.C. Zhu, Y.T. Qian, *China. J. Inorg. Chem.* 7 (2011) 1393.
19. H. Ma, W.Q. Ji, X.J. Yang, Z.L. Tao, J. Chen, *Sci. China. Chem.* 39 (2009) 918.
20. Z.Z. He, J.I. Yamaura, Y. Ueda, W.D. Cheng, *J. Solid State Chem.* 182 (2009) 2526.
21. M. Sánchez-Andújar, S. Yáñez-Vila, J. Mira, N. Biskup, J. Rivas, S. Castro-García, M.A. Señaris-Rodríguez, *J. Appl. Phys.* 109 (2011) 054106.
22. A.Q. Pan, J.G. Zhang, Z.M. Nie, G.Z. Cao, B.W. Arey, G.S. Li, S.Q. Liang, J. Liu, *J. Mater. Chem.* 20 (2010) 9193.
23. A.Q. Pan, J. Liu, J.G. Zhang, G.Z. Cao, W. Xu, Z.M. Nie, X. Jie, D.W. Choi, B.W. Arey, C.G. Wang, S.Q. Liang, *J. Mater. Chem.* 21 (2011) 1153.
24. A.Q. Pan, J.G. Zhang, G.Z. Cao, S.Q. Liang, C.G. Wang, Z.M. Nie, B.W. Arey, W. Xu, D.W. Liu, J. Xiao, G.S. Li, J. Liu, *J. Mater. Chem.* 21 (2011) 10077.
25. S.Q. Liang, J. Zhou, A.Q. Pan, Y.J. Li, T. Chen, Z.M. Tian, H.B. Ding, *Mater. Lett.* 74 (2012) 176.
26. X.G. Gao, P. Ruiz, Q. Xin, X.X. Guo, B. Delmon, *Catal Lett.* 23 (1994) 321.
27. J.M. Song, Y.Z. Lin, H.B. Yao, F.J. Fan, X.G. Li, S.H. Yu, *ACS Nano* 3 (2009) 653.
28. J. Xie, G.S. Cao, X.B. Zhao, M.J. Zhao, Y.D. Zhong, L.Z. Deng, Y.H. Guan, Z.T. Wu, *J. Mater. Sci.* 39 (2004) 1105.
29. P.G. Bruce, B. Scrosati, J.M. Tarascon, *Angew. Chem. Int. Ed.* 47 (2008) 2930.
30. N. Sivakumar, S.R.P. Gnanakan, K. Karthikeyan, S. Amaresh, W.S. Yoon, G.J. Park, Y.S. Lee, *J. Alloys Compd.* 509 (2011) 7038.
31. H. Qiao, Z. Zheng, L.Z. Zhang, L.F. Xiao, *J. Mater. Sci.* 43 (2008) 2778.
32. F.Y. Cheng, J. Chen, *J. Mater. Chem.* 21 (2011) 9841.
33. Z.X. Yang, G.D. Du, Z.P. Guo, X.B. Yu, Z.X. Chen, T.L. Guo, H.K. Liu, *J. Mater. Chem.* 21 (2011) 8591.